Materials Science and Engineering C 79 (2017) 140–150

Contents lists available at ScienceDirect

Materials Science and Engineering C

journal homepage: www.elsevier.com/locate/msec

Formulation and *in-vitro* efficacy of antifungal mucoadhesive polymeric matrices for the delivery of miconazole nitrate

G. Tejada [a], G.N. Piccirilli [a,b], M. Sortino [c,d], C.J. Salomón [a,e,*], M.C. Lamas [a,e], D. Leonardi [a,e,*]

[a] IQUIR-CONICET, Suipacha 570, 2000 Rosario, Argentina
[b] Área Bromatología y Nutrición, Departamento de Ciencias de los Alimentos y del Medio Ambiente, Facultad de Ciencias Bioquímicas y Farmacéuticas, Universidad Nacional de Rosario, Suipacha 570, 2000 Rosario, Argentina
[c] Área Farmacognosia, Departamento Química Orgánica, Facultad de Ciencias Bioquímicas y Farmacéuticas, Universidad Nacional de Rosario, Suipacha 570, 2000 Rosario, Argentina
[d] Centro de Referencia de Micología (CEREMIC), Facultad de Ciencias Bioquímicas y Farmacéuticas, Universidad Nacional de Rosario, Suipacha 570, 2000 Rosario, Argentina
[e] Área Técnica Farmacéutica, Departamento Farmacia, Facultad de Ciencias Bioquímicas y Farmacéuticas, Universidad Nacional de Rosario, Suipacha 570, 2000 Rosario, Argentina

ARTICLE INFO

Article history:
Received 31 January 2017
Received in revised form 25 April 2017
Accepted 7 May 2017
Available online 08 May 2017

ABSTRACT

Oral candidiasis is the most common opportunistic infection affecting patients with the human immunodeficiency virus. Miconazole buccal tablets or miconazole gel are approved for the treatment of oropharyngeal candidiasis. However, buccal films present more flexibility and also offer protection for the wounded mucosa, reducing pain. Due to their small size and thickness, buccal films may improve patients' compliance, compared to tablets. Additionally, they may increase the relatively short residence time on the mucosa of oral gels, which are easily removed by saliva. Polymeric films loaded with miconazole nitrate were prepared by a casting/solvent evaporation methodology using chitosan, carbopol, gelatin, gum arabic, and alginate to form the polymeric matrices. The morphology of films was investigated by scanning electron microscopy; interactions between polymers were analyzed by infrared spectroscopy and drug crystallinity by differential thermal analysis and X-ray diffraction. Films were characterized in terms of thickness, folding endurance, tensile properties, swelling, adhesiveness, and drug release. Finally, the antifungal activity against cultures of the five most important fungal opportunistic pathogens belonging to *Candida* genus was investigated. The more appropriate formulations were those based on chitosan-gelatin and chitosan-carbopol which showed good mechanical properties and adhesiveness, a relative low swelling index, improved drug release, and showed better *in vitro* activity against *Candida* cultures than miconazole nitrate raw material. Thus, it will be possible to produce a new pharmaceutical form based on polymeric films containing chitosan and miconazole nitrate, which could be loaded with low drug concentration producing the same therapeutic effect against *Candida* cultures.

1. Introduction

Candidiasis is a well-known fungal infection caused by several species of *Candida*, including *Candida albicans*, *Candida glabrata*, *Candida tropicalis*, *Candida parapsilosis*, and *Candida krusei*. *Candida* strains reside as a commensal in the gastrointestinal and genitourinary tracts and in the oral and conjunctival flora. Despite the fact that these yeasts are harmless to healthy individuals, most people with weakened immune systems are at risk of developing such fungal infections. Particularly, oral candidiasis is an opportunistic infection encountered in the population of patients with acquired immunodeficiency syndrome (AIDS) as well as in patients with hematological malignancies [1]. Even though antifungal drugs used in clinical treatments appear to be diverse and numerous, only a few are currently available to treat mucosal or systemic infections caused by *Candida* spp. Currently, azole antifungal agents including miconazole, econazole, clotrimazole, and ketoconazole are widely prescribed for antifungal therapy [1]. Recently, miconazole buccal tablets have been approved by the FDA for the treatment of oropharyngeal candidiasis. As reported, this formulation showed non-inferiority in the treatment of such infection compared with miconazole gel [2].

Although buccal devices containing antifungal compounds such as, buccal gel [3], bioadhesive buccal tablets [4], nanofiber mats [5] and patches [6–8] have been previously developed, buccal films present more flexibility and are able to protect the wounded mucosa, reducing pain. Furthermore, due to their small size and thickness, buccal films may improve patients' compliance if compared to tablets. Additionally, they may increase the relatively short residence time on the mucosa of oral gels, which are easily removed by saliva [9]. An ideal buccal film should possess good bioadhesive strength, flexibility, elasticity, softness and should also be adequately strong to withstand breakage due to stress from mouth activities. In general, buccal films are

* Corresponding authors at: Facultad de Ciencias Bioquímicas y Farmacéuticas, Universidad Nacional de Rosario, Suipacha 531, 24 (2000) Rosario, Argentina.
E-mail addresses: csalomon@fbioyf.unr.edu.ar (C.J. Salomón), leonardi@iquir-conicet.gov.ar (D. Leonardi).

http://dx.doi.org/10.1016/j.msec.2017.05.034
0928-4931/

composed of polymeric matrices. Several bioadhesive polymers including chitosan (CH), cellulose derivatives, pectins, poly (vinyl alcohol), and poly (vinyl pyrrolidone) are commonly used to prepare thin films. In many cases, the desired film properties may be achieved by mixing two or more polymers [10–12]. In this context, films based on CH-hydroxypropyl methylcellulose (HPMC) and CH-pectin (PC) for the delivery of miconazole nitrate were developed by our group [13]. It was observed that CH in combination with the non-ionic polymer showed smoother morphology, higher elongation to break, swelling index, and release of miconazole from the matrix than CH in combination with pectin [13]. These differences were mainly based on the matrix interactions due to the combination of "charged/non-charged" or "charged/charged" polymers. In addition, it has been postulated that the interaction between two oppositely charged polymers results in the formation of a complex, termed as polyelectrolyte complex. Different matrices of CH, a cationic polymer, with anionic polymers including carbopol (CB), gelatin (GEL), gum arabic (GA) and alginate (ALG) have been extensively studied, and some of them, used as potential carriers for the delivery of therapeutic agents [12,14–20]. For instance, matrices of CH and CB have been developed to facilitate the vaginal delivery of econazole nitrate [12], to prepare an extended-release matrix tablet containing theophylline [21], and to be used as potential skin drug delivery systems [22]. Matrices of CH and GEL have been developed for buccal delivery of propranolol hydrochloride [23], and have been evaluated as a postoperative adhesion barrier in rat cecum model [24]. They have also been formulated as bi-layer films with potential antimicrobial activity [25], and used to release tramadol hydrochloride [26]. Matrices of CH and GA have been developed and its formation analyzed according to the pH and ionic strength [27], and applied to produce nanoparticles loaded with insulin [18]. Moreover, matrices of CH and ALG have been extensively used as bioadhesive vaginal tablets [19] and for the implant delivery of vancomycin [20], among others. Those polymers have good mucoadhesive properties, which makes them suitable candidates for the design of bioadhesive buccal dosage forms [28]. By modifying the composition of the polyelectrolyte complexes, different charge densities may interact in various degrees, producing films with different mechanical properties, adhesiveness, swelling degree, morphology, drug release, and *in vitro* activity. Thus, according to the particular properties of CH, CB, GEL, GA and ALG, the main objective of this work was to develop buccal mucoadhesive films for the treatment of oral candidiasis, based on the formation of polylectrolyte complexes. The factors affecting the formulation of miconazole nitrate films, including bioadhesive and mechanical properties, swelling degree, dissolution rate and solid-state characterization, were analyzed. Additionally, the antifungal efficacy of these formulations based on CH and anionic polymers with different charge density, was investigated against cultures of the five most important fungal opportunistic pathogens belonging to *Candida* genus.

2. Materials and methods

2.1. Materials

CH (230 KDa average molecular weight and 80.6% of *N*-deacetylation) was supplied by Aldrich Chemical Co. (Milwaukee, WI, USA), GA (Mw = 250KDa), GEL (type A from pork skin, 125 Bloom value) and MN pharmaceutical grade were purchased from Parafarm, (Buenos Aires, Argentina). Sodium ALG (Sigma-Aldrich Co. Buenos Aires, Argentina), CB (Carbopol ® 971NF) by Lubrizol Advanced Materials, Inc. (Cleveland, OH, USA). All other chemicals were of analytical grade.

2.2. Methods

2.2.1. Film formulation

Formulation of films was based on the ionic interaction between CH and four anionic polymers: CB, GEL, GA and ALG.

CH solutions (3% w/v) were prepared dispersing CH in a solution of 10% v/v lactic acid (pH = 2.67) [29]. Aqueous solutions of CB (1.5% w/v), ALG (1.5% w/v), GEL (3.0% *w/v*), and GA (3.0% w/v) were prepared, stirred overnight and filtered through Miracloth® (Calbiochem-Novabiochem Corp., San Diego, CA). Then, CH solutions were dripped over each polymeric solution under magnetic stirring (Boecco stirrer, Germany) at 80 °C to avoid precipitation. MN (2% w/w) was solubilized in PEG 400, employed as a plasticizer (30% w/w) [30] and added to the polymeric solutions. The mixtures were stirred at 200 rpm for 2 h. Then, the solutions were cast on 9 cm diameter Petri dishes and dried (72 h at 40 °C, and 58% relative humidity (RH)). After being dried, films were neutralized in casting by addition of a phosphate buffer pH = 6.8 solution, washed with distilled water, and dried again [31]. Dried films were removed from the Petri dishes and conditioned in a chamber (72 h at 25 °C and 58% RH). The films used in the different tests were selected based on the lack of physical defects such as cracks, bubbles, and holes. The formulated films are described in Table 1.

2.2.2. Film characterization

2.2.2.1. Film thickness and folding endurance. For each film, six thickness measurements were made (around and in the center of the film) with a digital micrometer (Schwyz, China) [31]. Folding endurance was determined by repeatedly folding the films at the same place until they broke or were folded 300 times [32].

2.2.2.2. Mechanical properties. The mechanical strength of the films was evaluated by using an Universal Testing Machine Instron, single column, Series 3340 (Instron, Norwood, MA, United States) with a 10 N load cell. Films for each mechanical test were conditioned (24 h at 25 °C and 58% RH) and cut into strips (7 mm wide and 60 mm long) to evaluate tensile properties. The strip ends were mounted with double-sided tape and squares of 30 mm of cardstock to prevent tearing and slippage in the testing device (the exposed film strip length between cardstock ends was 30 mm). The initial grip distance was 30 mm and the crosshead speed was 0.05 mm/s. The parameters obtained from stress/strain curves were tensile strength (calculated by dividing the peak load by the cross-sectional area of the initial film), and elongation (calculated as the percentile of the change in the length of film with respect to the original distance between the grips). For each mechanical probe, three replicate measurements were performed.

Table 1
Film composition.

Composition					
CH	CB	GEL	GA	ALG	MN
100%					2% w/w
50%	50%				2% w/w
	100%				2% w/w
50%		50%			2% w/w
		100%			2% w/w
50%			50%		2% w/w
			100%		2% w/w
50%				50%	2% w/w
				100	2% w/w
100%					–
50%	50%				–
	100%				–
50%		50%			–
		100%			–
50%			50%		–
			100%		–
50%				50%	–
				100%	–

2.2.2.3. In vitro mucoadhesive strength. The mucoadhesive strength of the films was evaluated *in vitro* using an Instron universal testing machine. The adhesiveness of each film was obtained by measuring the force required to detach each formulation from a disk of porcine gum (obtained from "Paladini" slaughterhouse, V.G. Galvez, Argentina). Gums discs (2.5 cm diameter) were obtained by cutting the porcine gum with a punch biopsy. A portion of each film (2.5 cm diameter) was added to the upper end of the cylindrical probe and gum discs were horizontally attached to the lower end of the cylindrical probe by using double-sided adhesive tape. Prior to testing, discs were hydrated with artificial saliva (0.5 mL) for 5 min. Each film remained in contact with the gum disk for 5 min and then moved upwards at a constant speed of 1.0 mm/s. The test was carried out in triplicate. The force required to detach each film from the gum disk was determined from the resulting force/time plot [33].

2.2.2.4. Swelling index. Swelling measurements were determined by immersing an accurately weighed portion of the films (2.5 cm diameter obtained by a punch biopsy) in 0.5 mL of artificial saliva at 37 °C [34]. At predetermined time intervals (0, 5, 10, 15, 20, 30, 45, 60, 90, 120, 150, 180, 210, and 240 min), films were carefully removed, and the excess adhering moisture was gently blotted off and weighed. After that, 0.5 mL of artificial saliva was added again. The swelling index (SI) was calculated using the weights of dried (W_0) and swollen (W_t) films (Eq. (1)). The test was carried out in triplicate [31].

$$SI\ (\%) = W_t - W_0 / W_0 \times 100 \quad (1)$$

2.2.2.5. Scanning electron microscopy. Scanning electron microscopy (SEM, AMR 1000, Leitz, Wetzlar, Germany) was used to analyze the morphology of raw materials and films. A conductive and double-sided adhesive was employed to mount the film samples (previously cryo-fractured by immersion in liquid nitrogen) on an aluminum sample support. Samples were coated with a fine gold layer for 15 min at 70–80 mTorr in order to make them conductive before obtaining the SEM micrographs. Examinations were carried out using an accelerating voltage of 20 kV and magnification of 200×.

2.2.2.6. Fourier transform infrared spectroscopy. A FT-IR-Prestige-21 (Shimadzu, Tokyo, Japan) was used to obtain the Fourier transform infrared (FT-IR) spectra, using the KBr disk method (2 mg sample in 100 mg KBr) for the CH, CB, GEL, GA and ALG, and employing attenuated total reflectance with ZnSe crystal (ATR) for the film analysis. The scanning range was 700 to 3900 cm^{-1} with a resolution of 1 cm^{-1}.

2.2.2.7. Differential thermogravimetric analysis. Raw materials and films were investigated by the differential thermogravimetric analysis (DTG) method, using equipment having a high sensitive weight balance (Shimadzu DTG60). Samples consisting of MN (2 mg), or pieces of films (100 mg), were heated at a rate of 10 °C/min in the temperature range between 50 and 400 °C. All curves were normalized to unity of the initial sample mass.

2.2.2.8. X-ray diffraction. Data collection was carried out in transmission mode on an automated X'Pert Phillips MPD diffractometer (Eindhoven, The Netherlands). X-ray diffraction patterns were recorded using CuKα radiation (λ = 1.540562 Å), a voltage of 40 kV, a current of 20 mA and steps of 0.02° on the interval 2θ = 10°–50°.

Low peak broadening and background were assured by using parallel beam geometry by means of an X-ray lens and a graphite monochromator placed before the detector window. Data acquisition and evaluation were performed with the Stoe Visual-Xpow package, Version 2.75 (Germany).

2.2.2.9. Dissolution studies. Dissolution studies were performed in 900 mL of distilled water containing 1% v/v PEG 400 at 37 °C, using a USP XXIV apparatus (Hanson Research, SR8 8-Flask Bath, Ontario, Canada) with paddles rotating at 50 rpm. MN raw material was dispersed in the dissolution medium and films were fixed to the central shaft using cyanoacrylate adhesive [35]. Three samples of 5 mL each were taken using a filter at 0, 10, 20, 30, 40, 50 60, 90, 120, 180, 240 and 300 min. The amount of MN released was determined by UV spectrometry at 272 nm. An equal volume of the dissolution medium was added after each sample extraction to maintain a constant volume.

2.2.2.10. Halo zone test. Halo zone test was performed following the guidelines of disk diffusion method described in CLSI document M44-A2 [36]. *C. albicans* (ATCC 10231), *C. glabrata* (CCC115–00), *C. tropicalis* (CCC148–13), *C. parapsilosis* (ATCC 22019) and *C. krusei* (ATCC 6258) were cultured in Sabouraud's dextrose agar 18–24 h before testing. Testing was carried out on Agar plates (150 mm diameter) containing Mueller-Hinton agar, supplemented with 2% glucose (2 g/100 mL) and 0.5 μm/mL methylene blue (MB), at a depth of 4.0 mm. The inocula were prepared by suspending five distinct colonies in 5 mL of sterile distilled water and shaking on a vortex mixer for 15 s. The agar surface was inoculated by dipping sterile cotton swabs into a cell suspension adjusted to the turbidity of a 0.5 McFarland standard (approximately 1–5106 CFU/mL) and by streaking the plate surface in three directions. The plate was allowed to dry for 20 min, and then films were placed onto the surface of agar. Films containing 100% CH without drug and MN raw material were used as controls. The plates were incubated in air at 28 °C and read at 18 to 24 h. After 24 h of incubation, zone diameters (in millimeters) for the zone of complete inhibition were determined using a caliper and the mean value for each organism was recorded [37].

2.2.2.11. Statistical analysis. Analysis of variance was used and when the effect of the factors was significant the Tukey multiple ranks honestly significant difference test was applied (GraphPad Prism 5). Differences at $p < 0.05$ were considered significant.

3. Results and discussion

3.1. Films' thickness and mechanical properties

Films based only on CB showed high adhesiveness and flexibility, making them difficult to manipulate, while films based only on GEL or GA were found to be extremely brittle.

Since CB, GEL and GA were not suitable to formulate film matrices by themselves, the mechanical properties of those films were not analyzed.

Thickness determinations are essential to evaluate patient discomfort. Thickness value formulations ranged between 0.20 and 0.70 mm (Fig. 1a), which were adequated so as not to produce discomfort after application. However, a significant thickness variation was observed in films based on CH-ALG, producing different patterns of roughness. The interactions between strongly negatively charged polymers and CH may contribute to obtain the roughness variability pattern [12].

Formulated films based on CH-CB, CH-GEL, CH-GA and ALG showed the lowest thickness values ($p < 0.05$), which are adequate to avoid patient discomfort. Loaded and unloaded films exhibited almost identical values ($p > 0.05$).

Folding endurance is the number of times that a film can be folded at the same place without breaking or cracking. This study was done in order to evaluate film flexibility so that the film can be easily handled to produce comfort and a secured application. Films based only on ALG showed poor flexibility (folded 10 times before breaking). The rest of the film formulations (whether loaded or not with MN) were folded at least 300 times without breaking, indicating high mechanical strength. This property is highly desirable to avoid easy dislocation from the site of application or film breaking during administration [32].

CH films tensile strength values (Fig. 1b) were significantly improved when CH was combined with CB, GEL, and ALG ($p < 0.05$). The

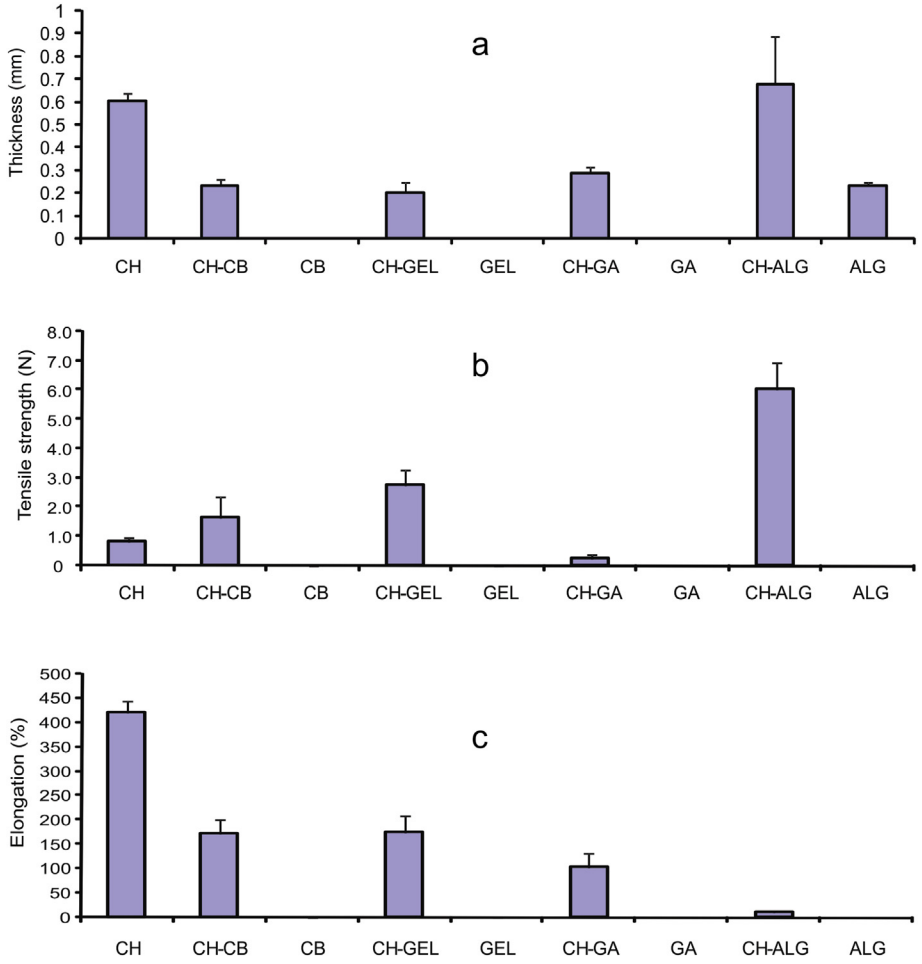

Fig. 1. Film characterization: (a) thickness, (b) tensile strength, (c) elongation to break.

interaction between anionic polymers and CH (ionic, electrostatic and/or hydrogen bonding) may bring about the improvement in the tensile strength. As can be observed, rigid matrices showed poor elasticity values (Fig. 1c), which may cause discomfort when applied [38]. The elongation of CH films decreased significantly when CH was in combination with the anionic polymers ($p < 0.05$). The combination CH-ALG showed the lowest elongation value. Therefore, after thoroughly analysing thickness, folding endurance, tensile strength and elongation properties, it can be suggested that the films based on CH, CH-CB and CH-GEL are the optimal choice.

3.2. In vitro mucoadhesive strength

Film mucoadhesive strength values are shown in Fig. 2. As can be observed, the adhesiveness of CH significantly increased ($p < 0.05$) when CH was in combination with CB, GEL, or ALG, while combinations with GA reduced the adhesiveness. *In vitro* mucoadhesive tests were performed to assess the ability, to adhere onto the gingivae. The highest increase in mucoadhesion strength was observed when CH was combined with CB. Hurler et al. reported that CB and CH solutions present similar bioadhesiveness [39]. However, in this work, when solutions were dried to obtain the films, those based only on CB showed extremely high adhesiveness and flexibility, making them difficult to manipulate and to analyze.

CH could interact with negatively charged surfaces. Interactions with mucin appear to be both electrostatic and/or hydrophobic [40]. Compared with non-ionic polymers, cationic and anionic polymers facilitate strong interaction with mucus [41].

The results of the present study indicate that the presence of charged functional groups in the polymeric chains render them as

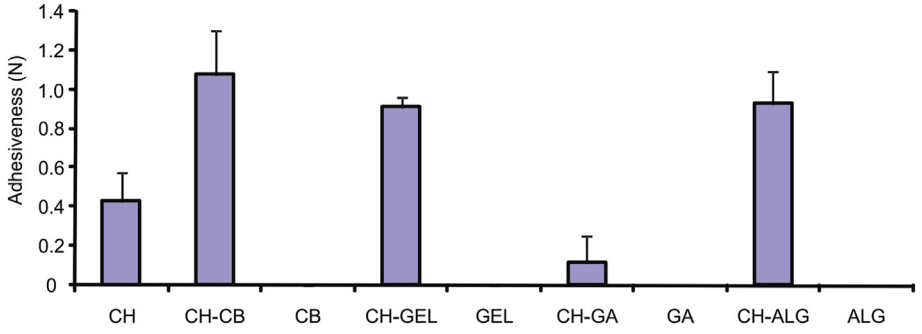

Fig. 2. Film mucoadhesive strength values.

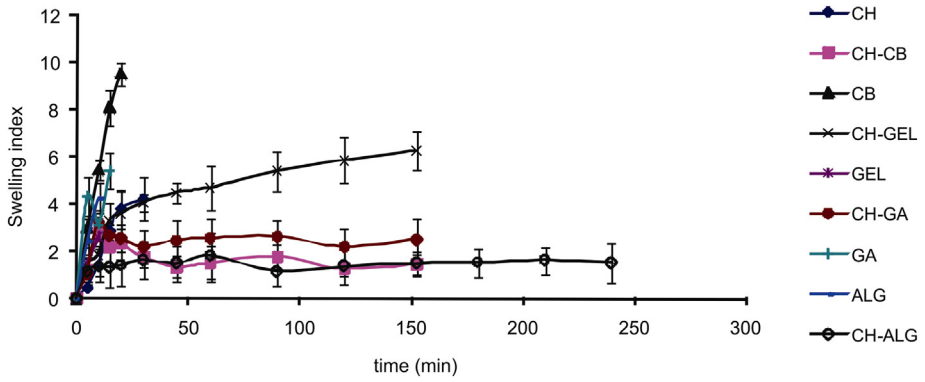

Fig. 3. Film swelling and disintegration in 0.5 mL of artificial saliva.

polyelectrolytes. Thus, the formation of strong hydrogen bonds and ionic interactions between the polymer functional groups and the mucosa has a clear effect on the strength of mucoadhesion layer as compared with the lowest charged polymer GA.

3.3. Swelling index

Films swelled in different ways depending on the polymer or polymer combination, used in the formulations (Fig. 3). Films based only on CB (swelling index 9.5), ALG (swelling index 8.4) or GEL (swelling index 6.3), were disintegrated after 30, 10 and 10 min respectively. Film based only on CH (swelling index 4.2) was disintegrated after 30 min. Films based on polymers with higher opposite charge density (CH-ALG and CH-CB) showed the lowest swelling index: 1.5 and 1.7 respectively, and were disintegrated between 150 and 240 min. Finally, films based on CH-GEL and CH-GA were disintegrated at 150 min and showed a swelling index of 2.8 and 6.2 respectively. As observed, swelling is strongly governed by the combination of the polymers. Fig. 3 clearly showed that the polymers themselves did not offer a suitable alternative to buccal drug delivery systems as their disintegration is too fast.

However, the combination between CH and GEL (CH-GEL films) delays the disintegration more than five times as compared with the polymers themselves. CH-GA and CH-CB films showed similar results, while CH-ALG films persisted without disintegration for 250 min.

The combination of CH with GEL, GA, CB and ALG produced a low mass equilibrium and an important increase in the disintegration time. It is possible to postulate that ionic interactions between the molecules induced stronger non-covalent binding leading films which are less swellable and which present a better structure to be administered for buccal treatments.

Additionally, a relationship between adhesiveness values and swelling at 5 min was observed (Fig. 4).

According to Peh & Wong, polymer swelling was reported to be an important factor in the bioadhesive behavior of the matrices [9]. Water retention capacity based on just one charged polymer can be categorized as superabsorbent and free carboxylic and amino groups play an important role in water uptake because of their hydrophilic nature [42]. On the other hand, in films based on combinations between oppositely charged polymers, the amino groups of CH interact with the carboxylic groups of the anionic polymers. These interactions probably reduced the number of amino groups and carboxylic free groups, diminishing the water retention capacity of these matrices and increasing the disintegration time.

Adhesion increased with the hydration degree after 5 min. However, an over-hydration observed in CB, GEL, GA and ALG (swelling index over 2) produced a complete loss of adhesiveness, probably due to the detachment originated at the polymer/tissue interface [9,43].

3.4. Scanning electron microscopy

SEM micrographs of MN, polymers and superficial sections of CH-GA, CH-GEL, CH-CB and CH-ALG films are shown in Fig. 5. MN (Fig. 5a) appears as irregular small crystals (10–20 μm). CH (Fig. 5b, 100–300 μm) with few smaller particles (20–40 μm), GEL (Fig. 5c, 100–500 μm), GA (Fig. 5d, 20–100 μm), and CB (Fig. 5e, 5–60 μm) are blocks with a smooth surface. ALG (Fig. 5f) appears as wrinkled blocks (50–300 μm with few smaller particles (20–60 μm)).

Films based on CH-GA showed a homogeneous and smooth surface (Fig. 5h) while CH-GEL (Fig. 5g) and CH-CB (Fig. 5i) films presented few signs of roughness. On the other hand, the CH-ALG films obtained by combination of strongly oppositely charged polymers exhibited

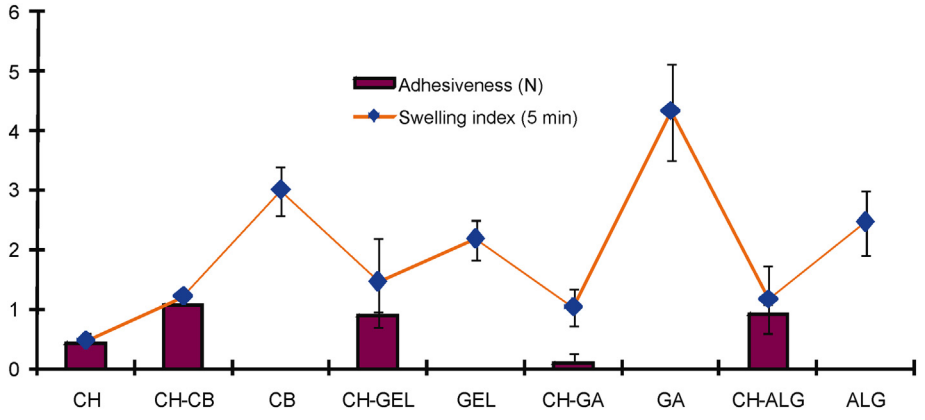

Fig. 4. Relationship between adhesiveness values and swelling at 5 min.

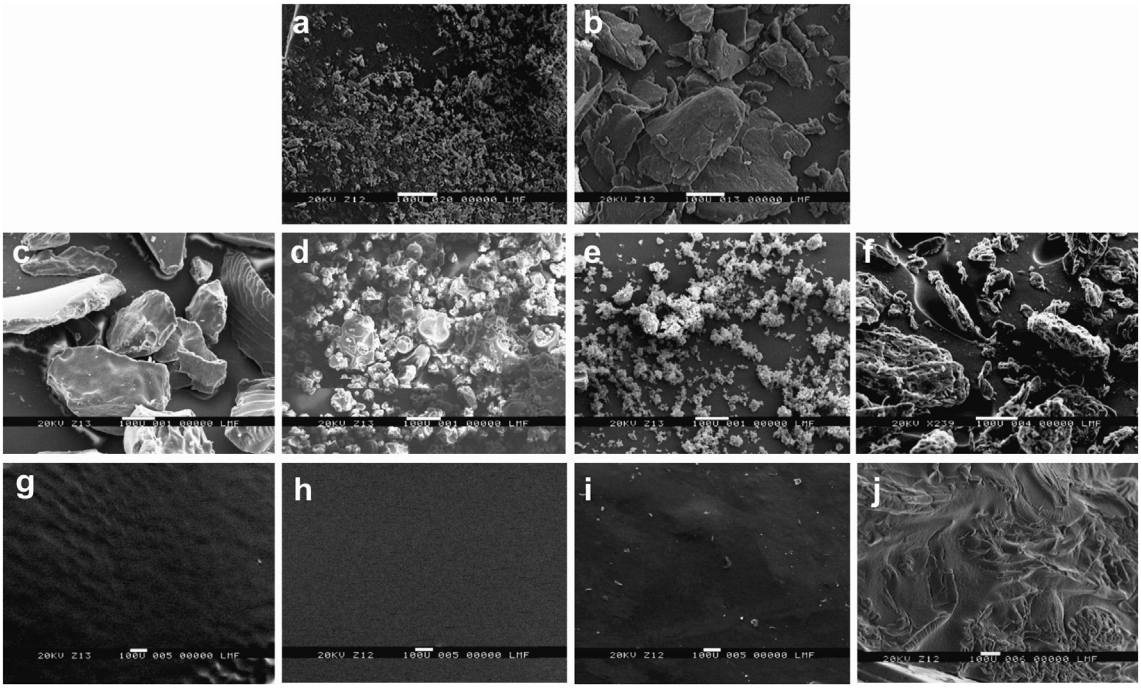

Fig. 5. Scanning electron microscopy micrographs of MN, polymers and superficial sections of films: a) MN, b) CH, c) GEL, d) GA, e) CB, f) ALG, g–j) film superficial sections, g) CH-GEL, h) CH-GA, i) CH-CB, j) CH-ALG.

different wrinkled patterns and cavities (Fig. 5j). It is important to remark that in CH-GA, CH-GEL, and CH-CB films, the structure was dense and compact, suggesting high structural integrity and good compatibility between the components [44].

3.5. Fourier transform infrared spectroscopy and differential thermogravimetric analysis

The interactions between the polymers were observed from the IR spectra. The CH spectrum showed a broad band with a maximum at 3450 cm^{-1}, assigned to the stretching vibration of O—H and N—H groups associated by intra and intermolecular hydrogen bonding; a characteristic absorption band at 2925 cm^{-1} assigned to the stretching vibration of the C—H bond; a band at 1643 cm^{-1} which correspond to the amide I; and two strong bands at 1595 cm^{-1} (NH_2 bending) [45] and 1420 cm^{-1}, due to stretching vibration of the carboxylic acid salt COO^- [46]; and finally a band at 1173 cm^{-1} which correspond to the amino groups [47]. The ALG spectrum showed asymmetric and symmetric stretching vibrations of the carboxylate salt ion at 1649 and 1460 cm^{-1} [48]. GA showed two strong bands at 1630 cm^{-1} and 1440 cm^{-1} due to asymmetric and symmetric stretching vibration of the carboxylic acid salt COO^- [46]. The GEL spectrum showed the COO stretching vibration peaks at 1680 cm^{-1} and 1640 cm^{-1} (amide I band), while the amide band II (N—H bending vibration) was observed at 1535 cm^{-1} [42,49]. Finally, the CB absorption band at 1708 cm^{-1} was assigned to the COO stretching vibration from carboxylic groups.

All films based on polymers combination showed a characteristic broad band at 3348 cm^{-1} in the infrared spectrum, corresponding to the O—H groups of the biopolymers, overlapped the stretching band of N—H. This broad band underlines the hydrogen bonding involved in the interaction between polymers. The C—H stretching vibration was observed at 2926 cm^{-1}. The IR spectra of films based on oppositely charged polymers changed significantly in the carbonyl-amide region. The NH_3^+ groups (CH band at 1595 cm^{-1}) and the asymmetric and symmetric COO^- stretching vibration at 1643 cm^{-1} and 1420 cm^{-1}, respectively, were shifted. Additionally, the C═O peaks of the anionic polymers were shifted: from 1649 to 1722 (ALG), from 1680 cm^{-1} to 1718 cm^{-1} (GEL), from 1708 to 1726 cm^{-1} (CB), and from 1630 to 1714 cm^{-1} (GA), indicating the interactions between the NH_3^+ groups of CH and the COO^- groups of all the other polymers [42,46,50]. Although several previous works have used this shifting as indicator of complex formation, it has also been reported that peaks appearing around 1720, 1458, 1242 and 1121 cm^{-1} could be due to the residual acid lactic and/or lactate used to obtain the films [51]. Therefore other changes were analyzed to ensure complex formation took place.

The CH-ALG spectrum (Fig. 6) was in good agreement with that obtained by Li et al. [47]. The amide I peak was shifted from 1643 to 1654 cm^{-1}, and the peak of the amino group (1173 cm^{-1}) was absent. These changes suggest the formation of the CH-ALG complex as a result of the ionic interaction between the negatively charged carbonyl groups (COO^-) of ALG and the positively charged amino groups (NH_3^+) of CH [47]. The CH-GA film spectrum showed that the amide I peak was shifted from 1643 to 1655 cm^{-1}. The NH_3^+ groups and asymmetric and symmetric COO^- stretching vibration at 1595 cm^{-1} and 1420 cm^{-1} disappeared, indicating an electrostatic interaction between the amine groups of CH (NH_3^+) and the carboxyl groups of GA (COO^-), which is in good agreement with previously reported data (46). In a similar way, the CH-GEL film spectrum showed that the amide I peak was shifted from 1643 to 1652 cm^{-1} and the NH_3^+ band and asymmetric and symmetric COO^- stretching vibration at 1600 cm^{-1} and 1420 cm^{-1} disappeared, indicating an electrostatic interaction between the amine groups of CH (NH_3^+) and carboxyl groups of GEL (COO^-). Finally, the IR spectrum of CH-CB showed that the peak of 1595 cm^{-1}, assigned to the amine band of CH, was shifted to 1640 cm^{-1} indicating that the amine group was protonated in the film. The bands at 1540 and 1415 cm^{-1} were assigned to the symmetric and asymmetric stretching of the COO^- group, indicating that the complex CH-CB was formed by an electrostatic interaction between the COO^- group of CB and the NH_3^+ group of CH [21].

The first derivative thermogravimetric analysis curves for raw MN and films are shown in Fig. 7. Pure MN presents a sharp endothermic peak at 186 °C, corresponding to the melting point of the crystalline

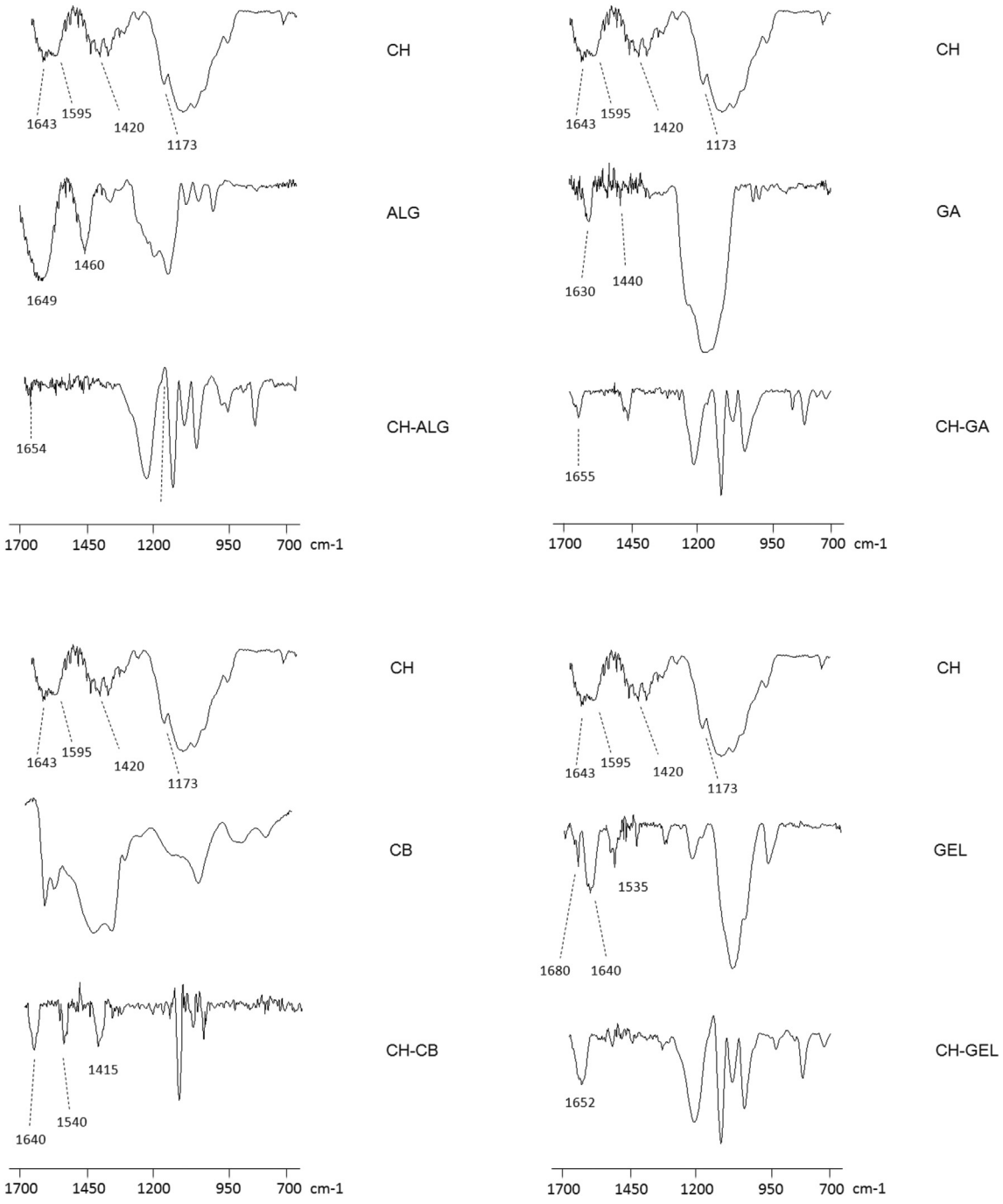

Fig. 6. Infrared spectra: polymers (raw materials) and films.

drug. MN endothermic peak disappeared in film thermograms, indicating that the drug was either molecularly dispersed in the polymeric matrix or that it was transformed from a crystalline to an amorphous state [52,53].

All starting polymers showed similar thermal degradation behavior. Curves presented endothermic peaks between 40 and 60 °C, attributed to water loss, followed by an exothermic peak between 250 and 300 °C, corresponding to polymer degradation [54]. It is clear that the water content in films was higher than that in powder raw materials. During films formulation, solutions of different polymers were mixed and then dried. However, the drying process was not carried out until constant weight, since had it been done that way, the mechanical properties of the films, such as elongation to break and adhesiveness would have declined.

Films based on oppositely charged polymers presented two endothermic peaks (80–100 °C and 150–210 °C), which may correspond to the evaporation of bound water in the polymeric matrices. Is has been reported that three different kinds of interactions between water and polymers in hydrogels may occur, presenting different endothermic peaks. The first peak, in the region 40–60 °C, corresponds to free water release; the second one, in the region 80–120 °C, corresponds to the release of water linked through hydrogen bonds; and finally the third peak, over 160 °C, is related to the release of water more tightly linked through polar interactions with carboxylate groups. As can be

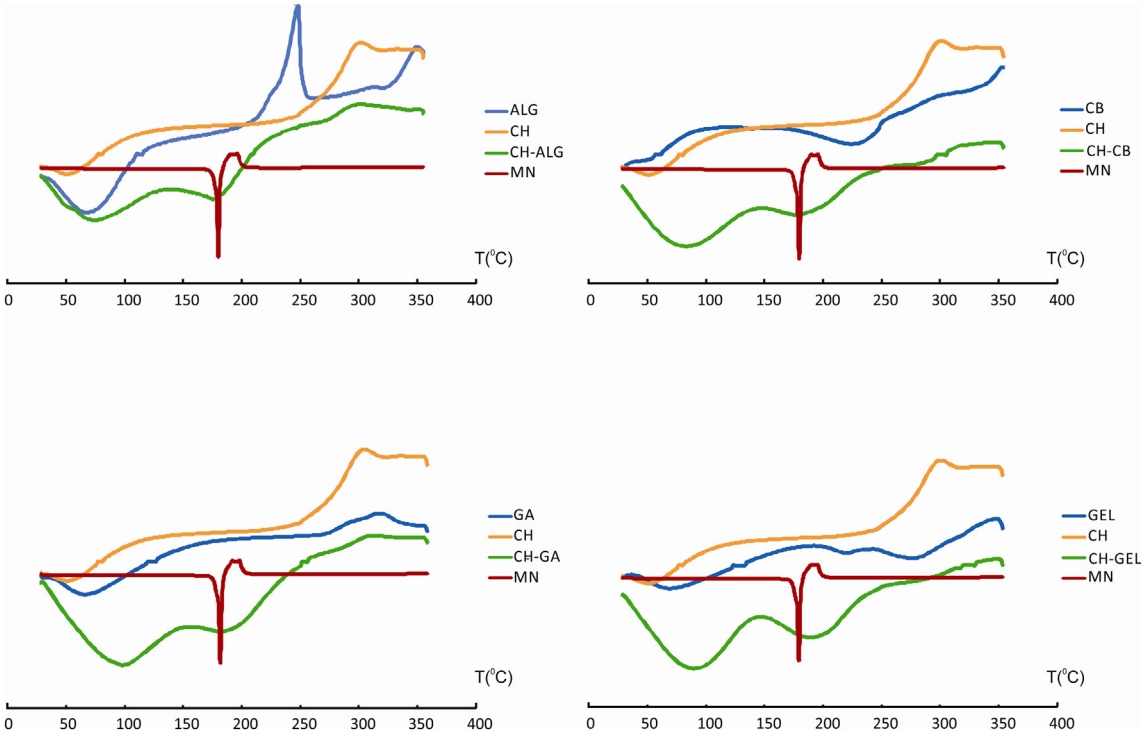

Fig. 7. Thermogravimetric analysis: first derivative curves for MN (raw material) and films.

observed in Fig. 7, films showed to have water linked both through hydrogen bonds and through polar interactions with carboxylate groups [54].

The thermal analyses showed that films are stable up to 100 °C for all the formulations, which is appropriate for oral films which will be applied on the oral mucosa (37 °C). Finally, it is to be noted that the

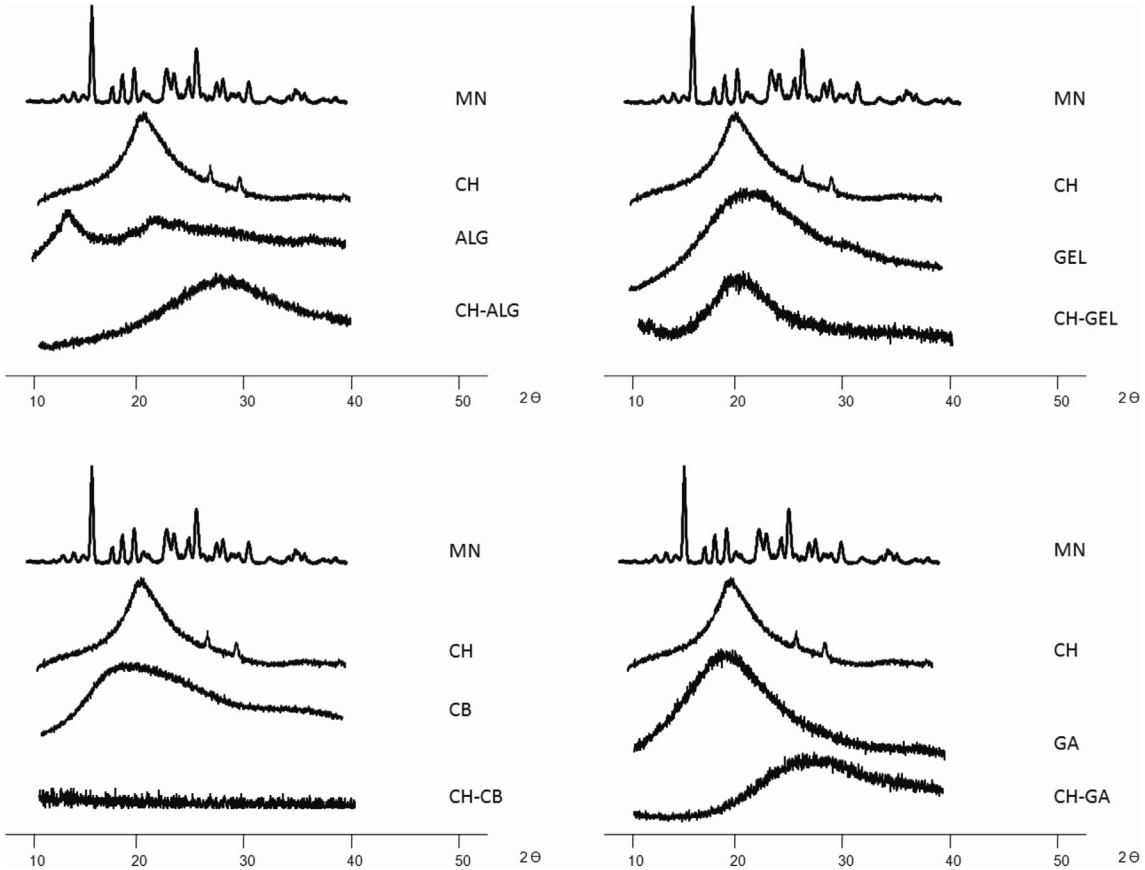

Fig. 8. X-ray diffraction patterns of MN raw material, polymers and films.

Table 2
Drug release values after 30, 60, 90 and 120 min (Q_{30}, Q_{60}, Q_{90}, and Q_{120}).

System	Q_{30} (%)	Q_{60} (%)	Q_{90} (%)	Q_{120} (%)
MN	3 ± 1	23 ± 2	35 ± 1	46 ± 3
CH-GA-MN	52 ± 2	99 ± 3	99 ± 2	99 ± 3
CH-ALG-MN	69 ± 4	99 ± 1	99 ± 2	100 ± 2
CH-CB-MN	73 ± 6	99 ± 1	100 ± 1	99 ± 2
CH-GEL-MN	64 ± 4	99 ± 2	100 ± 2	100 ± 1

Table 3
Antifungal activity of films (mean ± SD) after 24 h assay in cultures of *C. albicans*, *C. parapsilosis*, *C. tropicalis*, *C. krusei*, and *C. glabrata*.

Inhibition zone (mm)					
	C. albicans	*C. parapsilosis*	*C. tropicalis*	*C. krusei*	*C. glabrata*
CH-MN	32 ± 2	35 ± 3	36 ± 2	35 ± 3	33 ± 2
CH-GEL-MN	27 ± 3	44 ± 2	43 ± 2	35 ± 3	43 ± 3
CH-GA-MN	19 ± 2	21 ± 2	30 ± 1	18 ± 2	36 ± 2
CH-ALG-MN	33 ± 1	43 ± 3	46 ± 2	40 ± 3	37 ± 2
CH-CB-MN	26 ± 1	34 ± 2	32 ± 2	30 ± 2	37 ± 2
ALG-MN	23 ± 2	32 ± 2	34 ± 2	30 ± 2	36 ± 2
Test MN	19 ± 1	30 ± 1	20 ± 1	21 ± 1	25 ± 3
CH	6 ± 1	16 ± 2	8 ± 2	6 ± 1	18 ± 2

peak at about 300 °C, typical for pure CH, was not observed in films based on oppositely charged polymers, which seems to indicate interactions between polymers and may be considered as a proof of polymers complexation [54].

3.6. X-ray diffraction

The X-ray study was carried out to confirm the results of the thermogravimetric studies and to complete the characterization of the films. The X-ray patterns of MN raw material, polymers and films are shown in Fig. 8. The MN spectra showed sharp and narrow peaks at diffraction angles (2θ): 13.05°, 14.49°, 15.59°, 16.22°, 18.55°, 20.80°, 21.57°, 22.95°, 25.19°, 26.15°, 27.32°, 29.9°, 31.82°, 33.12°, 36.6°, 40.69°, with a typical crystalline pattern [55,56]. On the other hand, the X-ray spectra of the films did not show any peaks corresponding to crystalline MN. This is in concordance with the results obtained by DTG analysis showing that MN is in an amorphous state in the films or that the MN concentration in the films is below the detection limit [57].

The diffractograms of raw materials were in agreement with previously reported data. The raw CH showed a peak at around 20° related to the anhydrous CH crystals [58]. The diffractogram of ALG consisted of two crystalline peaks at 13.7° and 23.0°. GEL only had a typically wide crystalline peak at 21.8° [59] while GA showed a peak at 19.5° [60] and CB at 18° [61,62].

In the spectra of films based on oppositely charged polymers, the typical peak of CH disappeared, suggesting that the introduction of anionic polymers into CH disrupted the crystalline structure of CH. The amino and hydroxyl groups in CH form complexes with carboxylic groups of anionic polymers, which may break the hydrogen bonding between amino groups and hydroxyl groups in CH, resulting in an amorphous structure [58,63].

3.7. Dissolution studies

Films based on CH-GA, CH-GEL, CH-CB and CH-ALG improved the dissolution rate of MN. MN raw material showed 23% drug release after 60 min assay, while MN loaded films released >99%. The amorphous state of MN would be the main reason for the improvement in the dissolution rate of MN from the films.

Table 2 shows the drug release values after 30, 60, 90 and 120 min for each film and MN (Q_{30}, Q_{60}, Q_{90} and Q_{120}).

3.8. Halo zone test

Unloaded CH films and a paper disk containing MN were designed as controls. The unloaded CH film showed an inhibition zone (Table 3) that could be explained by the previously reported antimicrobial activity of CH, generating a matrix with antifungal properties.

The binding reaction between protonated CH amino groups with negatively charged cell surface molecules explains the antimicrobial activity of CH [64,65]. This theory is supported by the findings of Seyfarth et al., who reported that *N*-acetyl-D-glucosamine chitosan was unable to inhibit *C. albicans* and *C. krusei* growth and that it slightly reduced the growth of *C. glabrata* [66,67].

Films loaded with MN showed better activity after 24 h assay than MN (pure drug) ($p < 0.05$). The growth inhibition obtained from cultures of *C. albicans*, *C. glabrata*, *C. tropicalis*, *C. parapsilosis* and *C. krusei* are shown in Table 3. These results show that all films allowed MN release, and additionally, that MN may act in combination with the CH antimicrobial activity. Fig. 9a presents the growth inhibition as dark areas around the films for *C. glabrata* culture, and Fig. 9b shows comparison between the antifungal activities of MN pure drug, unload CH, CH-GEL-MN and CH-CB-MN films. The analysis of variance followed by Tukey test showed significant differences between the activity of CH-GEL-MN and MN pure drug ($p < 0.05$), and also between CH-GEL-MN and CH film ($p < 0.01$). The activity of MN against all assayed yeast was higher than the CH film ($p < 0.05$). Since the unloaded CH film did not show good activity against *C. albicans*, *C. tropicalis and C. krusei* no significant differences between MN pure drug and both CH-GEL-MN and CH-CB-MN films would be expected. Surprisingly, CH-GEL-MN and CH-CB-MN improved the MN activity ($p < 0.05$). This fact is probably related to the higher and faster dissolution of MN when it is

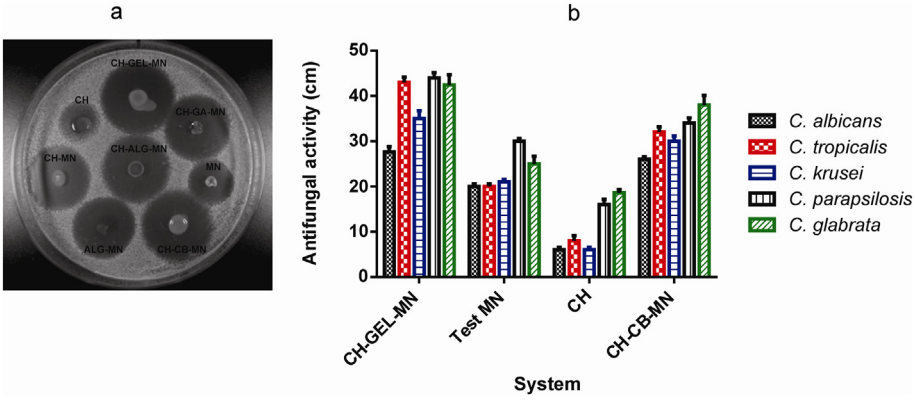

Fig. 9. a) Growth inhibition halos obtained around the films for *C. glabrata* culture b) Comparison between the antifungal activities of MN pure drug, unload CH, CH-GEL-MN and CH-CB-MN films.

in the films (Table 2), which may improve its diffusion in the agar medium. This increase in MN diffusion may explain the higher activity of the films with respect to MN pure drug.

Therefore, it would be possible to produce a new pharmaceutical form based on a polymeric film containing CH and MN, which could be loaded with a low drug concentration, and nevertheless, produce the same therapeutic effect against *Candida* cultures.

4. Conclusions

Nine different films loaded with MN employing five polymers were developed. CB, GEL and GA by themselves were not suitable to formulate films. Films based only on ALG showed poor flexibility and they were broken during the folding assay. Films based on CH-ALG were rigid and could produce patient discomfort. On the other hand, films based on CH-GA presented poor tensile strength and adhesiveness, indicating they may suffer an easy dislocation from the site of application. All the assayed films allowed a faster drug release rate than MN pure drug, probably due to the amorphous state of MN in the films, which is confirmed by DTG and X-ray diffraction. Film *in vitro* antifungal activity was assayed against the five most important fungal opportunistic pathogens belonging to *Candida* genus, showing a significant increase in MN activity when combined with CH. Based on these results, the most appropriate formulations were those based on CH-GEL and CH-CB. These films showed good mechanical properties and adhesiveness, a relatively low swelling index, improved drug release rate, and also showed better *in vitro* activity against *Candida* cultures than MN raw material.

Acknowledgements

The authors gratefully acknowledge the Universidad Nacional de Rosario (BIO 328), Argentina and CONICET (PIP 2015-2017-112 201501 00220) Argentina for financial support. We would like to thank the staff from the English Department (Facultad de Ciencias Bioquímicas y Farmacéuticas, Universidad Nacional de Rosario) for their assistance in the language correction of the manuscript.

References

[1] C. Spampinato, D. Leonardi, *Candida* infections, causes, targets, and resistance mechanisms: traditional and alternative antifungal agents, Biomed. Res. Int. 2013 (2013) 13.
[2] C.D. Collins, S. Cookinham, J. Smith, Management of oropharyngeal candidiasis with localized oral miconazole therapy: efficacy, safety, and patient acceptability, Patient Prefer Adherence 5 (2011) 369–374.
[3] A. De Pauw, T. De Backer, Miconazole buccal gel and risk for systemic bleeding: how certain topical formula can interfere with anticoagulants, Acta Clin. Belg. 70 (2) (2015) 121–123.
[4] C. Orvain, M.P. Moles-Moreau, S. François, M. Mercier, F. Moal, J.F. Hamel, et al., Miconazole mucoadhesive buccal tablet in high-dose therapy with autologous stem cell transplantation (HDT/ASCT)-induced mucositis, Support Care Cancer 23 (2) (2015) 359–364.
[5] P. Tonglairoum, T. Ngawhirunpat, T. Rojanarata, R. Kaomongkolgit, P. Opanasopit, Fabrication of a novel scaffold of clotrimazole-microemulsion-containing nanofibers using an electrospinning process for oral candidiasis applications, Colloids Surf. B: Biointerfaces 126 (2015) 18–25.
[6] N.A. Nafee, F.A. Ismail, N.A. Boraie, L.M. Mortada, Mucoadhesive buccal patches of miconazole nitrate: in vitro/in vivo performance and effect of ageing, Int. J. Pharm. 264 (1–2) (2003) 1–14.
[7] J. Van Roey, M. Haxaire, M. Kamya, I. Lwanga, E. Katabira, Comparative efficacy of topical therapy with a slow-release mucoadhesive buccal tablet containing miconazole nitrate versus systemic therapy with ketoconazole in HIV-positive patients with oropharyngeal candidiasis, J. Acquir. Immune Defic. Syndr. 35 (2) (2004) 144–150.
[8] P. Tonglairoum, T. Ngawhirunpat, T. Rojanarata, S. Panomsuk, R. Kaomongkolgit, P. Opanasopit, Fabrication of mucoadhesive chitosan coated polyvinylpyrrolidone/cyclodextrin/clotrimazole sandwich patches for oral candidiasis, Carbohydr. Polym. 132 (2015) 173–179.
[9] K.K. Peh, C.F. Wong, Polymeric films as vehicle for buccal delivery: swelling, mechanical, and bioadhesive properties, J. Pharm. Pharm. Sci. 2 (2) (1999) 53–61.
[10] D. Sakloetsakun, D. Preechagoon, A. Bernkop-Schnurch, T. Pongjanyakul, Chitosan-gum arabic polyelectrolyte complex films: physicochemical, mechanical and mucoadhesive properties, Pharm. Dev. Technol. 21 (5) (2016) 590–599.
[11] Y. Luo, Q. Wang, Recent development of chitosan-based polyelectrolyte complexes with natural polysaccharides for drug delivery, Int. J. Biol. Macromol. 64 (2014) 353–367.
[12] D.A. Real, M.V. Martinez, A. Frattini, M. Soazo, A.G. Luque, M.S. Biasoli, et al., Design, characterization, and in vitro evaluation of antifungal polymeric films, AAPS PharmSciTech 14 (1) (2013) 64–73.
[13] G. Tejada, M.G. Barrera, G.N. Piccirilli, M. Sortino, A. Frattini, C.J. Salomón, et al., Development and evaluation of buccal films based on chitosan for the potential treatment of oral candidiasis, AAPS PharmSciTech (2017) 1–11.
[14] M.-H. Lee, M.-K. Chun, H.-K. Choi, Preparation of Carbopol/chitosan interpolymer complex as a controlled release tablet matrix; effect of complex formation medium on drug release characteristics, Arch. Pharm. Res. 31 (7) (2008) 932–937.
[15] N.A. Gujarathi, B.R. Rane, J.K. Patel, pH sensitive polyelectrolyte complex of O-carboxymethyl chitosan and poly (acrylic acid) cross-linked with calcium for sustained delivery of acid susceptible drugs, Int. J. Pharm. 436 (1-2) (2012) 418–425.
[16] T. Guo, J. Zhao, J. Chang, Z. Ding, H. Hong, J. Chen, et al., Porous chitosan-gelatin scaffold containing plasmid DNA encoding transforming growth factor-β1 for chondrocytes proliferation, Biomaterials 27 (7) (2006) 1095–1103.
[17] J. Venkatesan, J.-Y. Lee, D.S. Kang, S. Anil, S.-K. Kim, M.S. Shim, et al., Antimicrobial and anticancer activities of porous chitosan-alginate biosynthesized silver nanoparticles, Int. J. Biol. Macromolec. 98 (2017) 515–525.
[18] M.R. Avadi, A.M.M. Sadeghi, N. Mohammadpour, S. Abedin, F. Atyabi, R. Dinarvand, et al., Preparation and characterization of insulin nanoparticles using chitosan and Arabic gum with ionic gelation method, Nanomedicine: NBM 6 (1) (2010) 58–63.
[19] A. El-Kamel, M. Sokar, V. Naggar, Gamal S. Al, Chitosan and sodium alginate—based bioadhesive vaginal tablets, AAPS PharmSci 4 (4) (2002) 224–230.
[20] Y. Mao, M. Zhao, Y. Ge, J. Fan, Novel alginate–chitosan composite microspheres for implant delivery of vancomycin and in vivo evaluation, Chem. Biol. Drug Des. 88 (3) (2016) 434–440.
[21] S.-H. Park, M.-K. Chun, H.-K. Choi, Preparation of an extended-release matrix tablet using chitosan/Carbopol interpolymer complex, Int. J. Pharm. 347 (1) (2008) 39–44.
[22] C.L. Silva, J.C. Pereira, A. Ramalho, A.A.C.C. Pais, J.J.S. Sousa, Films based on chitosan polyelectrolyte complexes for skin drug delivery: development and characterization, J. Membr. Sci. 320 (1–2) (2008) 268–279.
[23] A. Abruzzo, F. Bigucci, T. Cerchiara, F. Cruciani, B. Vitali, B. Luppi, Mucoadhesive chitosan/gelatin films for buccal delivery of propranolol hydrochloride, Carbohydr. Polym. 87 (1) (2012) 581–588.
[24] E. Shahram, S.H. Sadraie, G. Kaka, H. Khoshmohabat, M. Hosseinalipour, F. Panahi, et al., Evaluation of chitosan–gelatin films for use as postoperative adhesion barrier in rat cecum model, IJS 11 (10) (2013) 1097–1102.
[25] M. Pereda, A. Ponce, N. Marcovich, R. Ruseckaite, J. Martucci, Chitosan-gelatin composites and bi-layer films with potential antimicrobial activity, Food Hydrocoll. 25 (5) (2011) 1372–1381.
[26] S.K. Basu, K. Kavitha, M. Rupeshkumar, Evaluation of ionotropic cross-linked chitosan/gelatin B microspheres of tramadol hydrochloride, AAPS PharmSciTech 12 (1) (2011) 28–34.
[27] H. Espinosa-Andrews, J.G. Báez-González, F. Cruz-Sosa, E.J. Vernon-Carter, Gum Arabic–chitosan complex coacervation, Biomacromolecules 8 (4) (2007) 1313–1318.
[28] N. Salamat-Miller, M. Chittchang, T.P. Johnston, The use of mucoadhesive polymers in buccal drug delivery, Adv. Drug Deliv. Rev. 57 (11) (2005) 1666–1691.
[29] K. Peh, T. Khan, H. Ch'ng, Mechanical, bioadhesive strength and biological evaluations of chitosan films for wound dressing, J. Pharm. Pharm. Sci. 3 (3) (2000) 303–311.
[30] A. Domján, J. Bajdik, K. Pintye-Hódi, Understanding of the plasticizing effects of glycerol and PEG 400 on chitosan films using solid-state NMR spectroscopy, Macromolecules 42 (13) (2009) 4667–4673.
[31] I.C. Libio, R. Demori, M.F. Ferrão, M.I.Z. Lionzo, N.P. da Silveira, Films based on neutralized chitosan citrate as innovative composition for cosmetic application, Mater. Sci. Eng., C 67 (2016) 115–124.
[32] A.M. Avachat, K.N. Gujar, K.V. Wagh, Development and evaluation of tamarind seed xyloglucan-based mucoadhesive buccal films of rizatriptan benzoate, Carbohydr. Polym. 91 (2) (2013) 537–542.
[33] C. Eouani, P. Piccerelle, P. Prinderre, E. Bourret, J. Joachim, In-vitro comparative study of buccal mucoadhesive performance of different polymeric films, Eur. J. Pharm. Biopharm. 52 (1) (2001) 45–55.
[34] C. Giovino, I. Ayensu, J. Tetteh, J.S. Boateng, An integrated buccal delivery system combining chitosan films impregnated with peptide loaded PEG-b-PLA nanoparticles, Colloids Surf. B: Biointerfaces 112 (2013) 9–15.
[35] XXII UP, XVII N, US Pharmacopeial Convention. Rockville, Md, 1990 1788–1789.
[36] Clinical and Laboratory Standards Institute W, PA, Method for Antifungal Disk Diffusion Susceptibility Testing of Yeasts. Approved Guideline, second ed., Approved Guideline Second Edition Document M44-A2, 2008.
[37] Y. Wang, X. Guo, R. Pan, D. Han, T. Chen, Z. Geng, et al., Electrodeposition of chitosan/gelatin/nanosilver: a new method for constructing biopolymer/nanoparticle composite films with conductivity and antibacterial activity, Mater. Sci. Eng., C 53 (2015) 222–228.
[38] H. Nagahama, H. Maeda, T. Kashiki, R. Jayakumar, T. Furuike, H. Tamura, Preparation and characterization of novel chitosan/gelatin membranes using chitosan hydrogel, Carbohydr. Polym. 76 (2) (2009) 255–260.
[39] J. Hurler, N. Škalko-Basnet, Potentials of chitosan-based delivery systems in wound therapy: Bioadhesion study, J. Funct. Biomater. 3 (1) (2012) 37–48.

[40] T. Gratieri, G.M. Gelfuso, E.M. Rocha, V.H. Sarmento, O. de Freitas, R.F.V. Lopez, A poloxamer/chitosan in situ forming gel with prolonged retention time for ocular delivery, Eur. J. Pharm. Biopharm. 75 (2) (2010) 186–193.
[41] S. Karki, H. Kim, S.-J. Na, D. Shin, K. Jo, J. Lee, Thin films as an emerging platform for drug delivery, Asian J. Pharm. Sci. 11 (5) (2016) 559–574.
[42] K. Pal, A.K. Banthia, D.K. Majumdar, Preparation and characterization of polyvinyl alcohol-gelatin hydrogel membranes for biomedical applications, AAPS PharmSciTech 8 (1) (2007), E142-E6.
[43] J.O. Morales, J.T. McConville, Manufacture and characterization of mucoadhesive buccal films, Eur. J. Pharm. Biopharm. 77 (2) (2011) 187–199.
[44] R.A. Espinel Villacrés, S.K. Flores, L.N. Gerschenson, Biopolymeric antimicrobial films: study of the influence of hydroxypropyl methylcellulose, tapioca starch and glycerol contents on physical properties, Mater. Sci. Eng., C 36 (2014) 108–117.
[45] F. Ma, P. Li, B. Zhang, X. Zhao, Q. Fu, Z. Wang, et al., Effect of solution plasma process with bubbling gas on physicochemical properties of chitosan, Int. J. Biol. Macromol. 98 (2017) 201–207.
[46] H. Espinosa-Andrews, O. Sandoval-Castilla, H. Vázquez-Torres, E.J. Vernon-Carter, C. Lobato-Calleros, Determination of the gum Arabic–chitosan interactions by Fourier transform infrared spectroscopy and characterization of the microstructure and rheological features of their coacervates, Carbohydr. Polym. 79 (3) (2010) 541–546.
[47] Z. Li, H.R. Ramay, K.D. Hauch, D. Xiao, M. Zhang, Chitosan–alginate hybrid scaffolds for bone tissue engineering, Biomaterials 26 (18) (2005) 3919–3928.
[48] H. Daemi, M. Barikani, Synthesis and characterization of calcium alginate nanoparticles, sodium homopolymannuronate salt and its calcium nanoparticles, Sci Iran. 19 (6) (2012) 2023–2028.
[49] C. Zhuang, F. Tao, Y. Cui, Anti-degradation gelatin films crosslinked by active ester based on cellulose, RSC Adv. 5 (64) (2015) 52183–52193.
[50] M.P. Tedesco, C.A. Monaco-Lourenço, R.A. Carvalho, Gelatin/hydroxypropyl methylcellulose matrices - polymer interactions approach for oral disintegrating films, Mater. Sci. Eng., C 69 (2016) 668–674.
[51] G. Lawrie, I. Keen, B. Drew, A. Chandler-Temple, L. Rintoul, P. Fredericks, et al., Interactions between alginate and chitosan biopolymers characterized using FTIR and XPS, Biomacromolecules 8 (8) (2007) 2533–2541.
[52] N.B. Dobaria, A.C. Badhan, R.C. Mashru, A novel itraconazole bioadhesive film for vaginal delivery: design, optimization, and physicodynamic characterization, AAPS PharmSciTech 10 (3) (2009) 951–959.
[53] S. Freiberg, X.X. Zhu, Polymer microspheres for controlled drug release, Int. J. Pharm. 282 (1–2) (2004) 1–18.
[54] J. Ostrowska-Czubenko, M. Gierszewska-Drużyńska, Effect of ionic crosslinking on the water state in hydrogel chitosan membranes, Carbohydr. Polym. 77 (3) (2009) 590–598.
[55] A. Gupta, H.K. Kar, Solid state compatibility studies of miconazole using thermal and spectroscopic methods, Adv. Anal. Chem. Instrum. 5 (3) (2015) 51–55.
[56] A. Ribeiro, A. Figueiras, D. Santos, F. Veiga, Preparation and solid-state characterization of inclusion complexes formed between miconazole and methyl-β-cyclodextrin, AAPS PharmSciTech 9 (4) (2008) 1102–1109.
[57] C. Leuner, J. Dressman, Improving drug solubility for oral delivery using solid dispersions, Eur. J. Pharm. Biopharm. 50 (1) (2000) 47–60.
[58] X. Li, H. Xie, J. Lin, W. Xie, X. Ma, Characterization and biodegradation of chitosan–alginate polyelectrolyte complexes, Polym. Degrad. Stab. 94 (1) (2009) 1–6.
[59] Z. Dong, Q. Wang, Y. Du, Alginate/gelatin blend films and their properties for drug controlled release, J. Membr. Sci. 280 (1–2) (2006) 37–44.
[60] C. Cozic, L. Picton, M.-R. Garda, F. Marlhoux, D. Le Cerf, Analysis of arabic gum: study of degradation and water desorption processes, Food Hydrocoll. 23 (7) (2009) 1930–1934.
[61] H.H.C.M. Gangurde, S. Tamizharasi, K. Senthilkumaran, T. Sivakumar, Formulation and evaluation of sustained release bioadhesive tablets of ofloxacin using 3 2 factorial design, J. Pharm. Investig. 1 (2011) 148–156.
[62] S. Sahoo, C.K. Chakraborti, S.C. Mishra, Qualitative analysis of controlled release ciprofloxacin/carbopol 934 mucoadhesive suspension, J. Adv. Pharm. Technol. Res. 2 (3) (2011) 195–204.
[63] J.-S. Ahn, H.-K. Choi, M.-K. Chun, J.-M. Ryu, J.-H. Jung, Y.-U. Kim, et al., Release of triamcinolone acetonide from mucoadhesive polymer composed of chitosan and poly(acrylic acid) in vitro, Biomaterials 23 (6) (2002) 1411–1416.
[64] M.Z. Elsabee, E.S. Abdou, Chitosan based edible films and coatings: a review, Mater. Sci. Eng., C 33 (4) (2013) 1819–1841.
[65] O. Inta, R. Yoksan, J. Limtrakul, Hydrophobically modified chitosan: a bio-based material for antimicrobial active film, Mater. Sci. Eng., C 42 (2014) 569–577.
[66] A. Palmeira-de-Oliveira, M. Ribeiro, R. Palmeira-de-Oliveira, C. Gaspar, S. Costa-de-Oliveira, I. Correia, et al., Anti-*Candida* activity of a chitosan hydrogel: mechanism of action and cytotoxicity profile, Gynecol. Obstet. Investig. 70 (4) (2010) 322–327.
[67] F. Seyfarth, S. Schliemann, P. Elsner, U.-C. Hipler, Antifungal effect of high-and low-molecular-weight chitosan hydrochloride, carboxymethyl chitosan, chitosan oligosaccharide and N-acetyl-D-glucosamine against *Candida albicans*, *Candida krusei* and *Candida glabrata*, Int. J. Pharm. 353 (1) (2008) 139–148.